Received: 20 June 2022 | Revised: 13 September 2022 | Accepted: 15 September 2022

DOI: 10.1111/mpp.13274

Molecular Plant Pathology WILEY

ORIGINAL ARTICLE

A broadly conserved fungal alcohol oxidase (AOX) facilitates fungal invasion of plants

Nathaniel M. Westrick[1,2] | Sung Chul Park[3] | Nancy P. Keller[1,3] | Damon L. Smith[1] | Mehdi Kabbage[1]

[1]Department of Plant Pathology, University of Wisconsin-Madison, Madison, Wisconsin, USA

[2]United States Department of Agriculture–Agricultural Research Service, Madison, Wisconsin, USA

[3]Department of Medical Microbiology and Immunology, University of Wisconsin-Madison, Madison, Wisconsin, USA

Correspondence
Mehdi Kabbage, Department of Plant Pathology, University of Wisconsin-Madison, Madison, WI, USA.
Email: kabbage@wisc.edu

Funding information
Agricultural Research Service, Grant/Award Number: 58-3060-8-023; National Institute of Food and Agriculture, Grant/Award Number: 2021-67011-35151 and Wis04031

Abstract

Alcohol oxidases (AOXs) are ecologically important enzymes that facilitate a number of plant–fungal interactions. Within Ascomycota they are primarily associated with methylotrophy, as a peroxisomal AOX catalysing the conversion of methanol to formaldehyde in methylotrophic yeast. In this study we demonstrate that AOX orthologues are phylogenetically conserved proteins that are common in the genomes of nonmethylotrophic, plant-associating fungi. Additionally, AOX orthologues are highly expressed during infection in a range of diverse pathosystems. To study the role of AOX in plant colonization, AOX knockout mutants were generated in the broad host range pathogen *Sclerotinia sclerotiorum*. Disease assays in soybean showed that these mutants had a significant virulence defect as evidenced by markedly reduced stem lesions and mortality rates. Chemical genomics suggested that SsAOX may function as an aromatic AOX, and growth assays demonstrated that Δ*SsAOX* is incapable of properly utilizing plant extract as a nutrient source. Profiling of known aromatic alcohols pointed towards the monolignol coniferyl alcohol (CA) as a possible substrate for SsAOX. As CA and other monolignols are ubiquitous among land plants, the presence of highly conserved AOX orthologues throughout Ascomycota implies that this is a broadly conserved protein used by ascomycete fungi during plant colonization.

KEYWORDS
alcohol oxidase, fungi, plant pathogen, *Sclerotinia sclerotiorum*

1 | INTRODUCTION

Fungal–plant associations are ancient, and probably facilitated the colonization of terrestrial systems by both kingdoms some 400 million years ago (Lutzoni et al., 2018). These associations have varied effects on the health of individual plants, from mutualistic to pathogenic, but in natural ecosystems fungi play a critical role in both carbon cycling and the maintenance of plant biodiversity (Zeilinger et al., 2016). Fungal species are often categorized for their supposed ecological niche in relation to plants (e.g., saprophytes, epiphytes, symbionts, pathogens), but these categories are rarely unambiguous, with many fungi transitioning between modalities in response to biotic and/or environmental conditions (Zeilinger et al., 2016).

Common fungal components of the plant phyllosphere are methylotrophic yeasts, including *Pichia pastoris*, which are notable as a rare group of eukaryotes capable of utilizing methanol as

a sole carbon source (Yurimoto et al., 2011). This activity is driven by the oxidation of methanol into formaldehyde, and subsequently into energy for the cell, by a peroxisomally localized alcohol oxidase (AOX) (Cregg et al., 1989). Such a localization is critical, as AOX generates toxic levels of hydrogen peroxide (H_2O_2) during the oxidation of methanol, which is subsequently degraded to water and oxygen by a peroxisomal catalase (CAT) (Yurimoto et al., 2011). Despite the rarity of true methylotrophy throughout the rest of the fungal kingdom, disparate reports of AOX orthologues have been noted in filamentous fungal species throughout the subphylum Pezizomycotina (phylum Ascomycota) (Holzmann et al., 2002; Isobe et al., 2007; Kubicek et al., 2014; Segers et al., 2001; Soldevila & Ghabrial, 2001). Broadly, these genes were characterized as likely methanol oxidases, despite their poor capacity to oxidize methanol and other short-chain alcohols and limited evidence that they function in methanol utilization on an organismal scale (Isobe et al., 2007; Segers et al., 2001). More recent analysis of the orthologous AOX from the common environmental fungus *Aspergillus terreus* suggests that these proteins demonstrate relatively poor activity on short-chain alcohols (i.e., methanol, ethanol, etc.), but are quite efficient in the oxidation of aromatic alcohols (Chakraborty et al., 2014). This finding is intriguing from the perspective of fungal–plant interactions, as aromatic alcohols are major constituents of structural lignin in plants (Sederoff et al., 1999). Interestingly, the implication of AOX orthologues in plant disease development has been demonstrated. In the plant pathogen *Passalora fulva* (formerly *Cladosporium fulvum*), genetic knockouts of *AOX* resulted in drastically reduced virulence (Segers et al., 2001). This leads to the possibility that AOXs may be involved in the degradation/consumption of plant components, including during pathogenic interactions, rather than simply in the utilization of methanol.

While discussions of AOXs within Ascomycota often focus on methylotrophy, AOXs from basidiomycetes are more often discussed for their role in lignin degradation (Galperin et al., 2016). Rather than localizing to the peroxisome, basidiomycete aromatic (aryl-) AOXs are secreted by the fungus and produce H_2O_2 through the cyclic oxidation of *p*-methoxybenzyl alcohol to *p*-anisaldehyde, thus facilitating the activity of a similarly secreted versatile peroxidase enzyme in attacking structural lignin (Hernández-Ortega et al., 2012). Although peroxisomal AOX activity is unlikely to operate on plant material through such a mechanism, it does provide precedence for the role of aromatic AOX in the degradation of specific plant components. The fungal degradation of plant material is an intricate process in which fungi secrete a repertoire of cell wall-degrading, proteolytic, and lipolytic enzymes in order to break down plant cellular/structural components (Kubicek et al., 2014). These elements are actively absorbed through membrane transporters and are converted to energy through a number of biochemical pathways. While this is typically thought to be a primarily metabolic process, the catabolic breakdown of these components is often necessary to avoid the accumulation of toxic intermediates in the fungal cell, suggesting that metabolism and detoxification are probably intertwined processes (Huisjes et al., 2012; Westrick et al., 2021; Zhang & van Kan, 2013).

In this study, we identified a specific AOX orthologue with a role that is distinct from the previously described methylotrophic and wood rotting niches, and with a wide distribution throughout the ascomycete subphylum Pezizomycotina. We investigated the structural and phylogenomic conservation of AOX genes within Pezizomycotina and demonstrate this protein's possible role in helping fungi to degrade the monomeric components of structural lignin. Using a combination of expression studies, reverse genetics analyses, and chemical genomics, we show that AOX is required for virulence in the model pathogen *Sclerotinia sclerotiorum*, by allowing the fungus to cope with and metabolize plant aromatic alcohols, and thus effectively colonize host tissues. These data represent a marked shift from the methylotrophy model previously associated with AOXs and propose that AOXs are broadly conserved proteins used by ascomycete fungi to promote the colonization of plant tissues.

2 | RESULTS

2.1 | AOX is broadly conserved within Ascomycota and preferentially maintained in plant-colonizing species

To determine the prevalence of AOX orthologues throughout the phylum Ascomycota, 314 fungal genomes within the National Center for Biotechnology Information (NCBI) Reference Sequence (RefSeq) Protein Database were analysed for homology to *S. sclerotiorum* AOX (SsAOX). Approximately 60% (187/314) of the species analysed contained at least one putative SsAOX orthologue (Table S1; Figure S1). AOX early discovery and characterization in methylotrophic yeast suggested a mechanistic association with this relatively uncommon lifestyle. All six AOX-containing yeast species in either Saccharomycotina (6/68) or Taphrinomycotina (0/9) are known or suspected methylotrophs (Figure S1).

Remarkably, we found that AOX is comparatively more enriched in Pezizomycotina (181/236 assessed species), the subdivision containing filamentous ascomycetes and most known fungal plant pathogens (Figure S1). The protein sequence is also highly conserved, as nearly all copies found within Pezizomycotina contain greater than 76% amino acid identity with SsAOX (Figure 1a; Figure S1; Table S1). This conservation also extends to the predicted peroxisomal subcellular localization of the various AOX proteins (Figure 1b,c; Tables S1 and S2). It has been demonstrated that evolutionarily conserved genes preferentially accumulate introns, so an analysis of intron density within Pezizomycotina genera containing AOX orthologues was performed (Carmel et al., 2007). While an average fungal gene contains up to two introns, *AOX* orthologues have an unusually high intron content (2–16), with most genera containing more than six (Figure S2, Table S3) (Csuros et al., 2011; Kupfer et al., 2004). A separate study analysing splice form variation in *S. sclerotiorum* did not find that *SsAOX* is subject to alternative splicing across multiple hosts, suggesting that these introns probably are

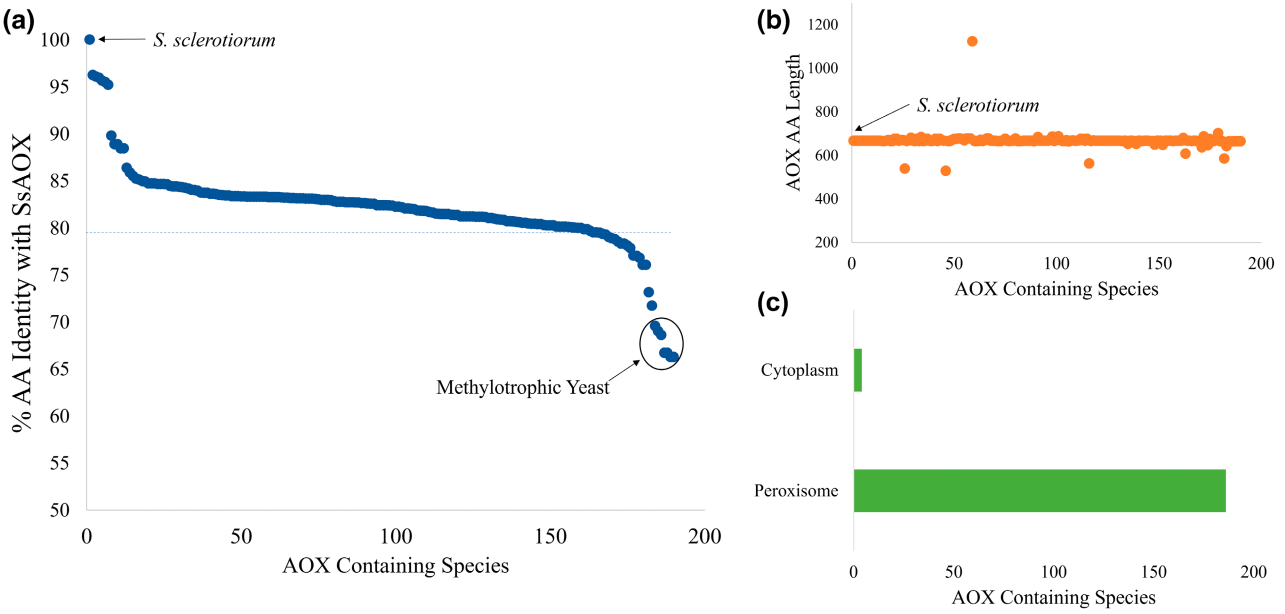

FIGURE 1 Characteristics of AOX orthologues throughout the phylum Ascomycota. (a) Percentage amino acid (AA) identity of distinct ascomycete AOX orthologues with *Sclerotinia sclerotiorum* alcohol oxidase (SsAOX). (b) AA length of AOX orthologues within the phylum Ascomycota. (c) Predicted subcellular localization of ascomycete AOX orthologues.

not present to maintain multiple isoforms of the protein (Ibrahim et al., 2021). This supports the theory that there has been strong evolutionary pressure to limit mutations and structurally conserve AOX, which is further supported by protein modelling demonstrating a nearly identical structure of AOX across filamentous ascomycetes (Figure S3).

As the list of species being analysed is probably biased towards specific genera (e.g., *Aspergillus*) and lifestyles (e.g., pathogens) that have been highly sequenced, and such a bias may overstate the value of AOX in certain ecological niches. A phylogenetic tree was generated from species in our data set to evaluate gene conservation/loss (Figure 2a). From this tree we can observe at least 18 distinct AOX gene loss events within Pezizomycotina. To contextualize these gene loss events, we consider that phylogenomic evidence suggests that the most recent common ancestor of Pezizomycotina probably consumed plant hydrocarbons and may have been a pathogen of early plants (Sanchez-Rodríguez et al., 2010). In more recent millennia many species within Pezizomycotina have transitioned away from dependence on plant-derived carbon, and strikingly the loss of AOX appears to largely coincide with such transitions (Figure 2b; Table S4). While AOX has been maintained in the genome of nearly all plant pathogens in our data set (74/80), it has been lost in the genomes of all primary animal pathogens (0/25) (e.g., *Pseudogymnoascus destructans*, *Coccidioides immitis*, *Metarhizium* spp.) and some species that are found primarily on animal faecal matter (e.g., *Eremomyces bilateralis*, *Chaetomium thermophilum*) (Table S4). Of the plant pathogens that have lost AOX, most are known biotrophs (e.g., *Ustilagodinea virens*, *Blumeria* spp., *Claviceps purpurea*) that acquire plant nutrients through specialized interactions with live plant cells rather than through the active destruction and digestion of plant cellular material seen during fungal saprotrophy and necrotrophy (Figure 2b; Table S4) (Kubicek et al., 2014). These gene loss events suggest that the loss of AOX strongly correlates with a shift in carbon acquisition strategy away from plant material. Such a correlation is further supported by the loss of AOX in true plant endophytes such as *Epichloe* spp. and *Xylona hevea* and the lichen *Endocarpon pusillum* (Figure 2b; Table S4) (Becker et al., 2016; Gazis et al., 2016).

Other gene loss events in Pezizomycotina are less easily explained, including the striking number of opportunistic animal pathogens that are missing *AOX* (26/43) across six distinct clades (Figure 2b; Table S4). It is unlikely that such loss is correlated with an active evolution towards animal association, as opportunistic pathogens typically adapted to multiple environments, but may be associated with a broadening ecological niche related with some opportunists (Vicente et al., 2017).

2.2 | *AOX* is up-regulated during infection across multiple pathosystems

While *AOX* appears to be maintained in the genomes of most plant-pathogenic ascomycetes, it is important to establish its specific expression during plant colonization/pathogenesis. To assess the importance of AOX during plant infection, *AOX* expression was analysed in multiple pathosystems. RNA sequencing data were collected from *S. sclerotiorum* during infection of soybean and chickpea (Mwape et al., 2021; Westrick et al., 2019), from *Botrytis cinerea* during infection of tomato fruit and the bryophyte *Physcomitrium patens* (Petrasch et al., 2019; Reboledo et al., 2021), from *Aspergillus flavus* during infection of peanut (Wang et al., 2016), from *Fusarium*

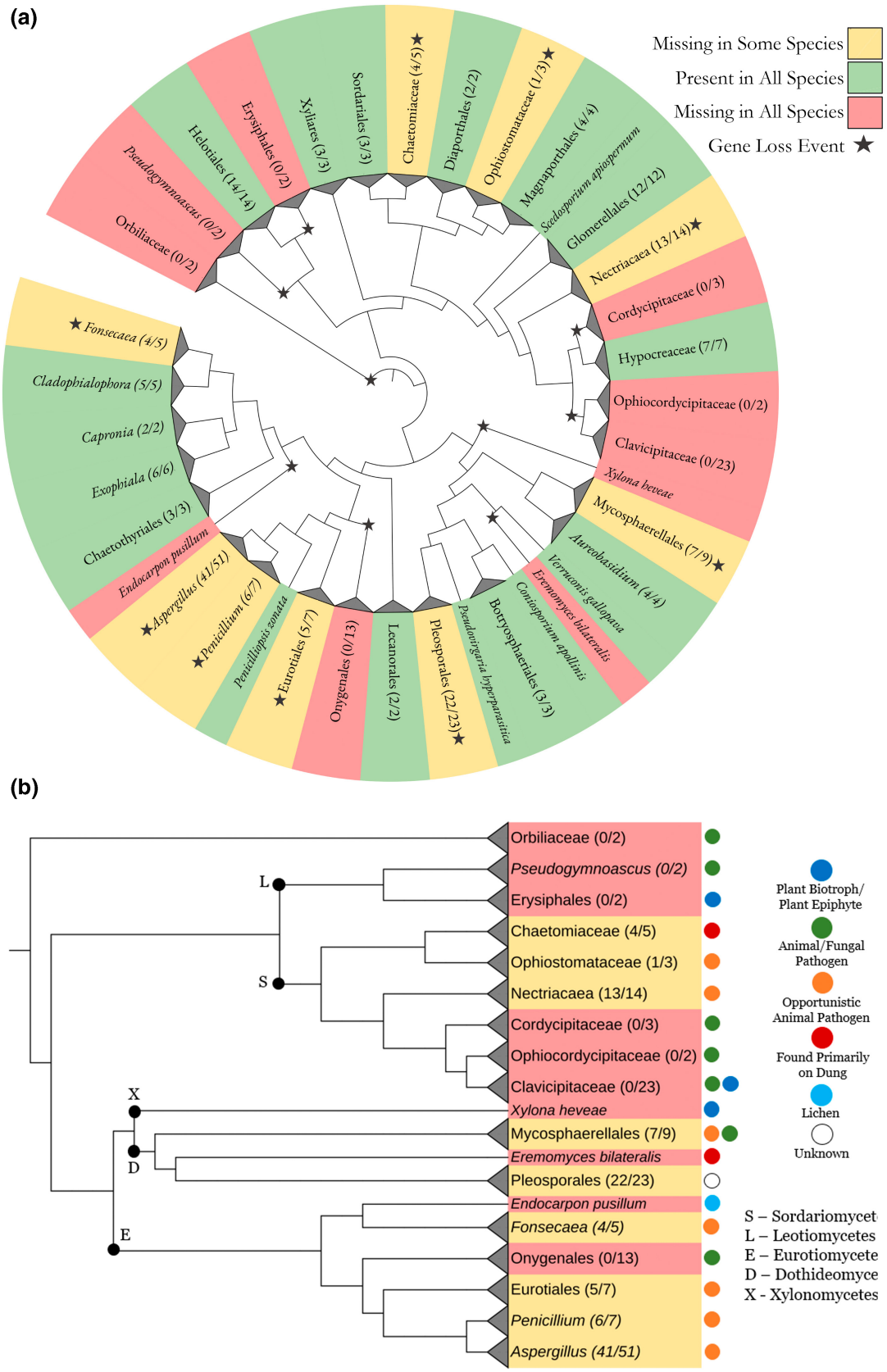

FIGURE 2 Phylogenetic analysis of *AOX* gene loss events. (a) Cladogram representing the evolutionary relationships of the 236 members of Pezizomycotina represented in the NCBI RefSeq protein database. Clades/species are coloured depending on the presence of *AOX* in all (green), none (red), or some (yellow) species. Stars indicate putative gene loss events. (b) Cladogram representing the clades/species that have lost *AOX* in some or all species. Coloured circles represent the ecological niche/lifestyles associated with species that have lost *AOX* (Table S4).

oxysporum during infection of cucumber (Huang et al., 2019), from *Fusarium graminearum* during infection of wheat (Puri et al., 2016), and from *Dothistroma septosporum* during infection of pine (Bradshaw et al., 2016) (Figure 3). These pathosystems allow for the analysis of AOX usage during infection of angiosperm (fruit, stem, and root), gymnosperm, and bryophyte tissue. Additionally, the fungal species contain representatives from the four major classes within Pezizomycotina: Eurotiomycetes (*A. flavus*), Sordariomycetes (*F. graminearum* and *F. oxysporum*), Leotiomycetes (*S. sclerotiorum* and *B. cinerea*), and Dothideomycetes (*D. septosporum*).

AOX expression in each pathosystem is represented as the fold change in expression when compared to a representative in vitro control (Figure 3). *AOX* was up-regulated during infection of all assessed pathosystems; expression levels largely increased over the course of infection, from relatively low to no expression at early timepoints to often >1000-fold induction at the later stages of infection (Figure 3). The two pathosystems in which *AOX* expression is more predominant during early infection are *B. cinerea*–tomato and *F. graminearum*–wheat, which are both interesting examples of post-harvest infections in which the pathogens are invading fruit rather than photosynthetic/structural plant material (Figure 3). A potential distinguishing factor behind these different expression patterns is that infection of either tomato fruit or wheat grains would require a pathogen to first contend with more lignified tissues prior to penetrating the more carbohydrate-rich interior (Andrews et al., 2002; Asthir et al., 2010). This runs contrary to many necrotrophic pathosystems in which we expect the pathogen to contend with increasingly lignified plant material and a greater concentration of monolignols over the progression of infection (Huang et al., 2019; Mwape et al., 2021; Westrick et al., 2019). To assess the relative importance of AOX within a specific pathogen across multiple hosts, we additionally evaluated the expression of *SsAOX* during the infection of six distinct hosts from publicly available transcriptomic data (Kusch et al., 2021). On all hosts *SsAOX* was found to be up-regulated between 200- and 5000-fold when compared to an in vitro control, suggesting that *SsAOX* is highly expressed during infection in a nonhost-specific manner (Kusch et al., 2021).

2.3 | *S. sclerotiorum* mutants lacking AOX are undermined in virulence and stem colonization

To assess the role of AOX during infection and development, the *S. sclerotiorum* AOX gene, *SsAOX*, was deleted using CRISPR/Cas9-mediated homologous recombination, replacing *SsAOX* with a hygromycin resistance cassette. No developmental defects were observed in the Δ*SsAOX* strains when grown on potato dextrose agar (PDA) (Figure S4). Pathogenicity assays were conducted by inoculating detached leaves and whole soybean plants with wild-type 1980 (WT) and Δ*SsAOX* mutant strains of *S. sclerotiorum*.

Lesions on soybeans infected with Δ*SsAOX* knockout strains were significantly smaller than on those infected with the WT on both detached leaves and stems when measured over the course of the assay (Figure 4a–c). Surprisingly, even at 9 days postinoculation

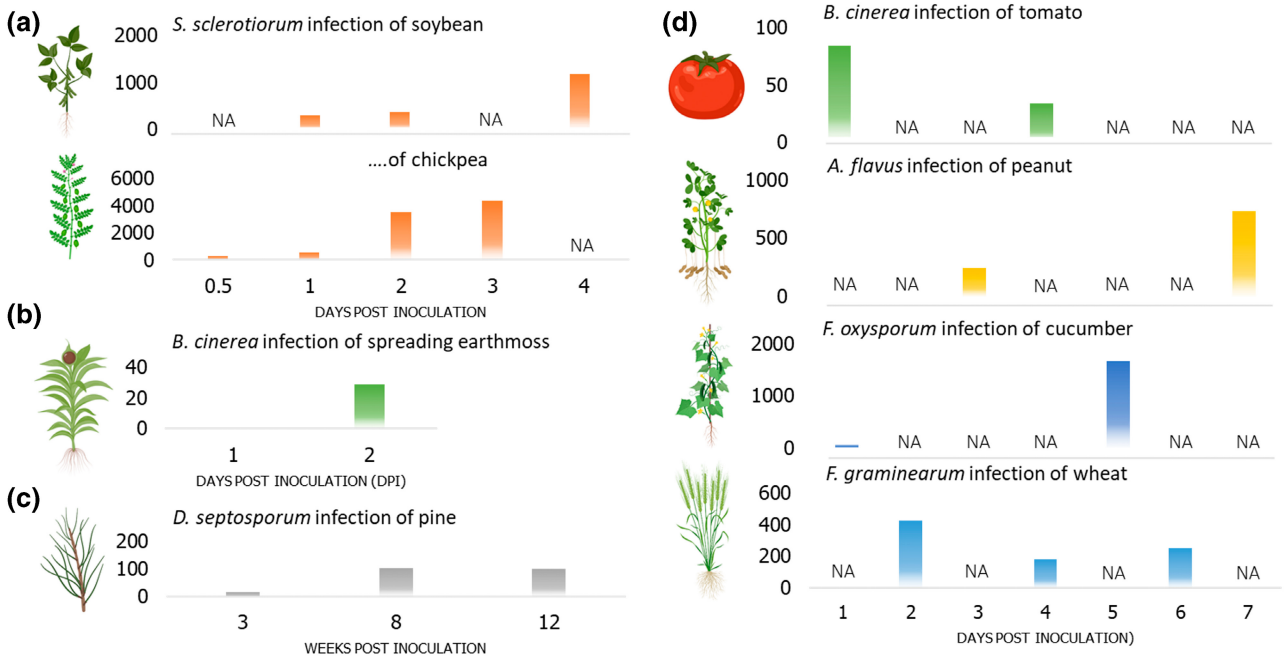

FIGURE 3 *AOX* expression across multiple pathosystems. The *y* axes represent the fold change in expression of distinct *AOX* orthologues in comparison to in vitro culture controls. NA represents no data for a given timepoint. Expression over (a) 4 days of infection (*Sclerotinia sclerotiorum*/chickpea [Mwape et al., 2021] and soybean [Westrick et al., 2019]), (b) 2 days of infection (*Botrytis cinerea*/*Physcomitrium patens* [Reboledo et al., 2021]), (c) 12 weeks of infection (*Dothistroma septosporum*/pine [Bradshaw et al., 2016]), and (d) 7 days of infection (*B. cinerea*/tomato [Petrasch et al., 2019], *Aspergillus flavus*/peanut [Wang et al., 2016], *Fusarium oxysporum*/cucumber [Huang et al., 2019], and *Fusarium graminearum*/wheat [Puri et al., 2016]).

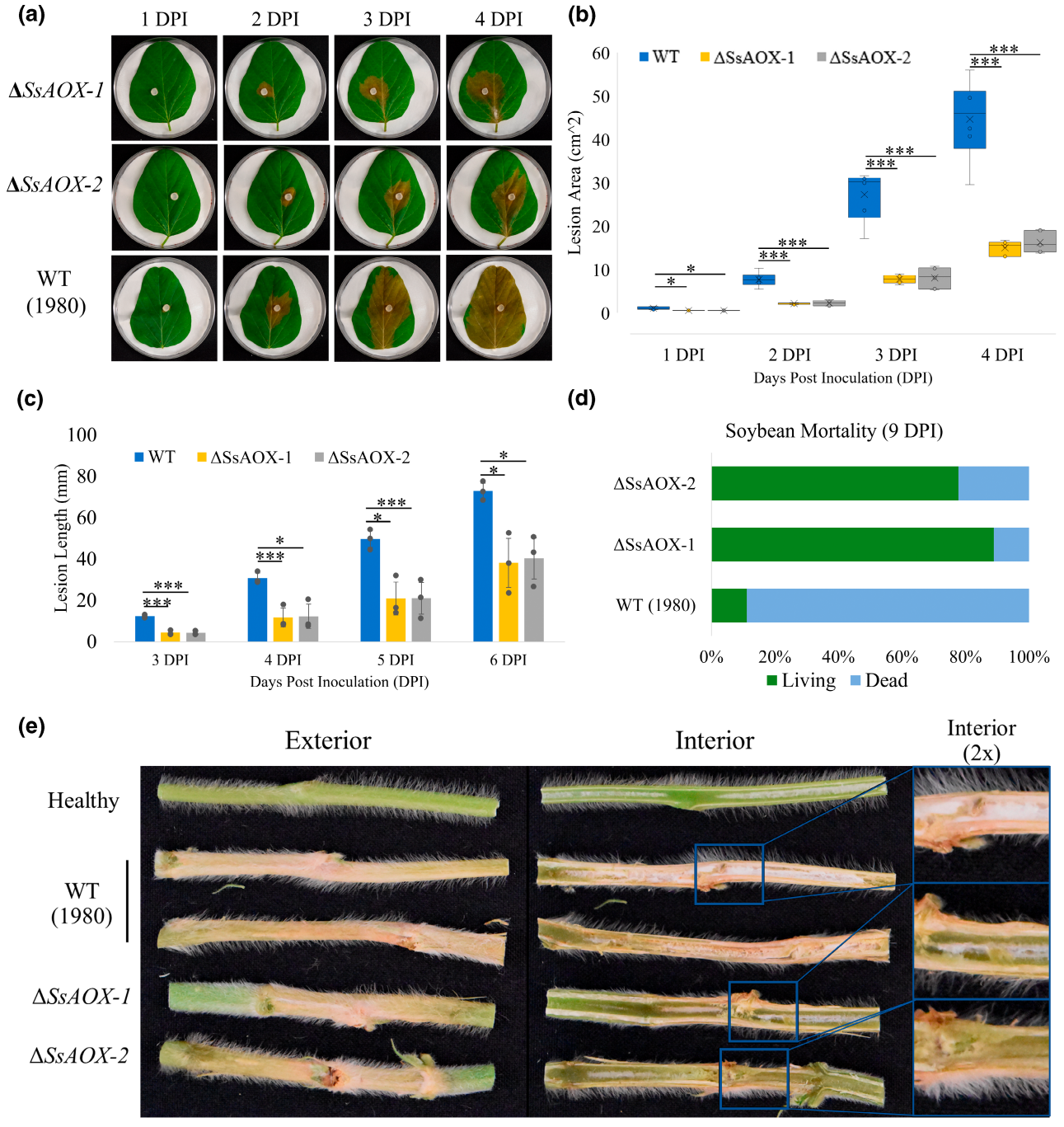

FIGURE 4 Disease assays of wild-type (WT) *Sclerotinia sclerotiorum* and Δ*SsAOX* mutants on soybeans. (a) Images of detached soybean leaves infected with either WT or Δ*SsAOX* mutants. (b) Lesion measurements of WT- or Δ*SsAOX*-infected soybean leaves. (c) Measurements of stem lesions on whole soybeans infected with WT or Δ*SsAOX* mutants through cut petioles. (d) Mortality of whole soybean plants infected with WT or Δ*SsAOX* mutants at 9 days postinoculation (DPI). (e) Interior and exterior of healthy, WT-infected, and Δ*SsAOX*-infected soybean stems. Error bars represent standard deviation. Statistical analysis was performed with a Student's *t* test on three to six biological replicates per assay. $^{*}p < 0.05$, $^{***}p < 0.001$.

whole plants inoculated with Δ*SsAOX* showed a noticeably lower mortality rate (about 11%–22%) than those infected with the WT (about 77%–89%) (Figure 4d; Figure S5). As *S. sclerotiorum* typically kills soybean plants by colonizing the vasculature within the main stem, WT and Δ*SsAOX* infected stems were collected for further evaluation (Figure 4e). Cross-sections of infected stems demonstrate that while both WT and Δ*SsAOX* appeared to develop similarly on the exterior cortex cells of the stem, the pith and central xylem cells of Δ*SsAOX* infected stems appeared largely unaffected. Contrary to this, the vasculature of WT infected stems was fully colonized by *S. sclerotiorum* (Figure 4e).

To assess the plant's response to both mutant and WT infections, inoculated soybean stems were subjected to gas chromatography–mass spectrometry (GC–MS) analysis. Despite

the induction of surface lesions by both strains, principal component analysis shows the metabolic profile of Δ*SsAOX*-infected stems clustering more closely with healthy tissue than that of WT-infected stems (Figure 5a). A closer look at metabolites associated with plant defence revealed a significant accumulation of defence compounds typically produced against necrotrophs in WT-infected tissue, including linolenic acid (the precursor to jasmonic acid), oleic acid, and nicotinamide (Figure 5b; Table S5) (He & Ding, 2020; Kachroo et al., 2008; Sidiq et al., 2021). Conversely, metabolites more typically associated with defence against hemibiotrophs and biotrophs were accumulated at significantly higher levels in Δ*SsAOX*-infected stems (Figure 5c) (Lenk et al., 2019). This is probably due to the less destructive nature of Δ*SsAOX* colonization. To assess this, we examined the accumulation of metabolites associated with the destruction of structural components such as plant cell walls. As predicted, we observed a far

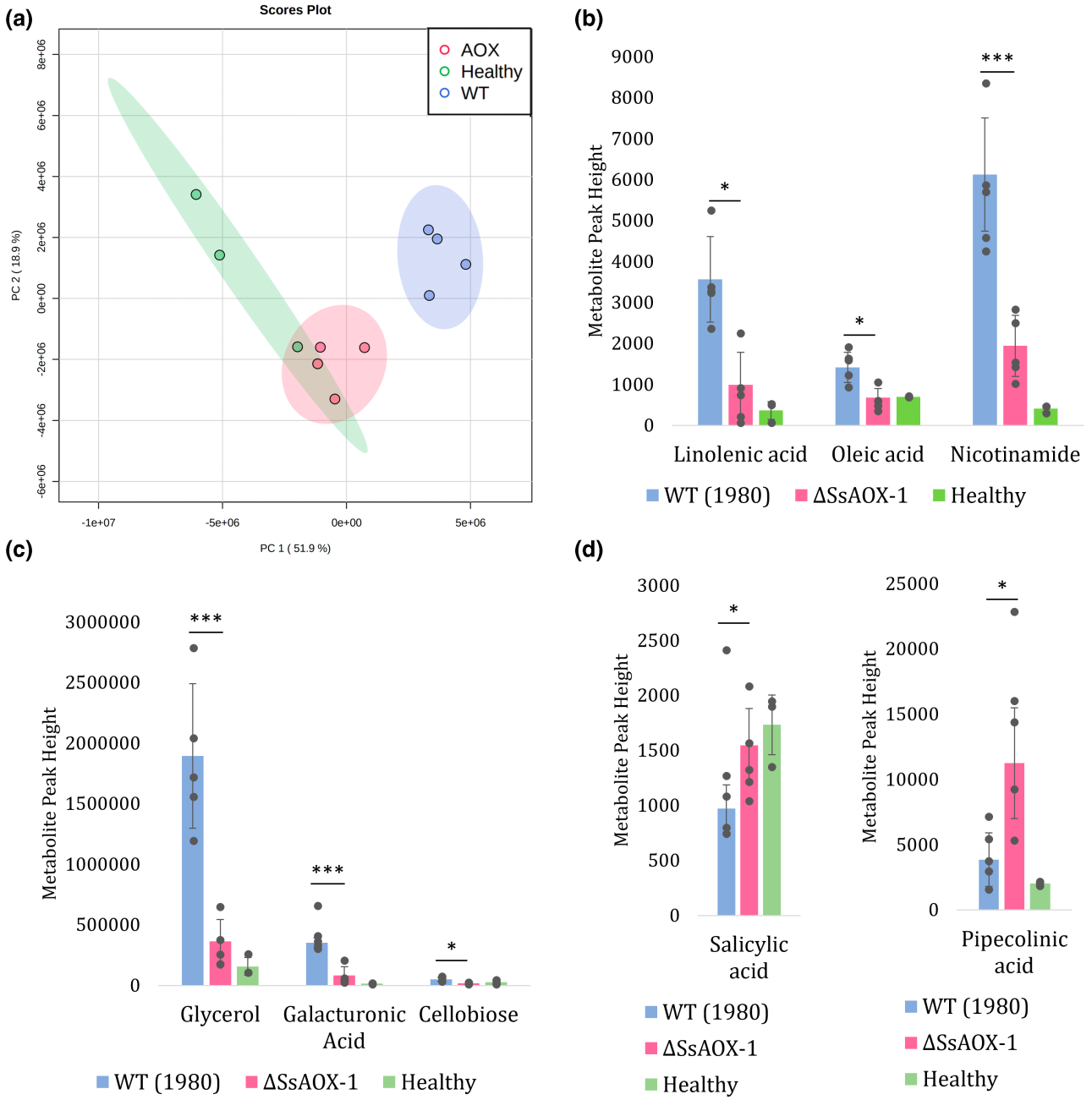

FIGURE 5 Gas chromatography–mass spectrometry analysis of healthy, wild-type (WT)-infected, and Δ*SsAOX* (Δ*SsAOX*-1)-infected soybean stems at 96 h postinoculation. (a) Principal component analysis comparing the metabolic profiles of the analysed samples. (b) Metabolites commonly associated with plant defence against necrotrophic infections (linolenic acid, oleic acid, and nicotinamide). (c) Accumulated plant cell wall and cell membrane components (glycerol, galacturonic acid, and cellobiose). (d) Metabolites commonly associated with plant defence against biotrophic infections (salicylic acid and pipecolinic acid). Error bars represent standard deviation. WT-infected stem ($n = 5$), Δ*SsAOX*-infected stem ($n = 5$), healthy stem ($n = 3$). Statistical analysis was conducted through comparison of WT- and Δ*SsAOX*-infected samples using a Student's *t* test, $^{*}p < 0.05$, $^{***}p < 0.001$.

greater accumulation of the cell wall/membrane constituents such as galacturonic acid (pectin), cellobiose (cellulose), and glycerol (phospholipids) in WT-infected plants (Figure 5d). This potential reduction in tissue maceration additionally helps to explain the altered lesion phenotype observed upon Δ*SsAOX* infection of older soybean leaves (Figure S6). In conclusion, our data demonstrate that *SsAOX* is an important virulence factor of *S. sclerotiorum* and probably other fungi, and contributes to the pathogen's capacity to properly colonize and exploit host tissues.

2.4 | AOX is critical for fungal utilization of specific plant metabolites

The virulence defect and altered metabolic profile of Δ*SsAOX* confirm the importance of SsAOX in successful infection; however, it is important to clarify whether SsAOX plays a role in detoxification/metabolism, subversion of host defences, or physical penetration. To assess its potential role in the metabolism of plant material, soybean stem extract (SE) was used to supplement 1% glucose minimal medium (GMM) for fungal growth assays. No significant difference in growth was observed between WT and Δ*SsAOX* when grown on GMM + 1% ethanol (control), but when grown in GMM + 1% SE the WT grew to nearly twice the mass of the control over a 3-day period (Figure 6a). Comparatively, Δ*SsAOX* appeared unresponsive to the addition of SE, a surprising result as SE is expected to contain a number of simple carbohydrates in addition to the phenolics known to be abundant in lignified plant material (Figure 6a). It is known that methylotrophic yeast use AOX for carbon acquisition when acting on alcohols (methanol) and for nitrogen acquisition when acting on simple amines (methylamine) (Yurimoto et al., 2011). To determine if this growth phenotype may be due to SsAOX facilitating nitrogen assimilation from SE, WT *S. sclerotiorum* was grown in minimal media with and without the addition of carbon/nitrogen and supplemented

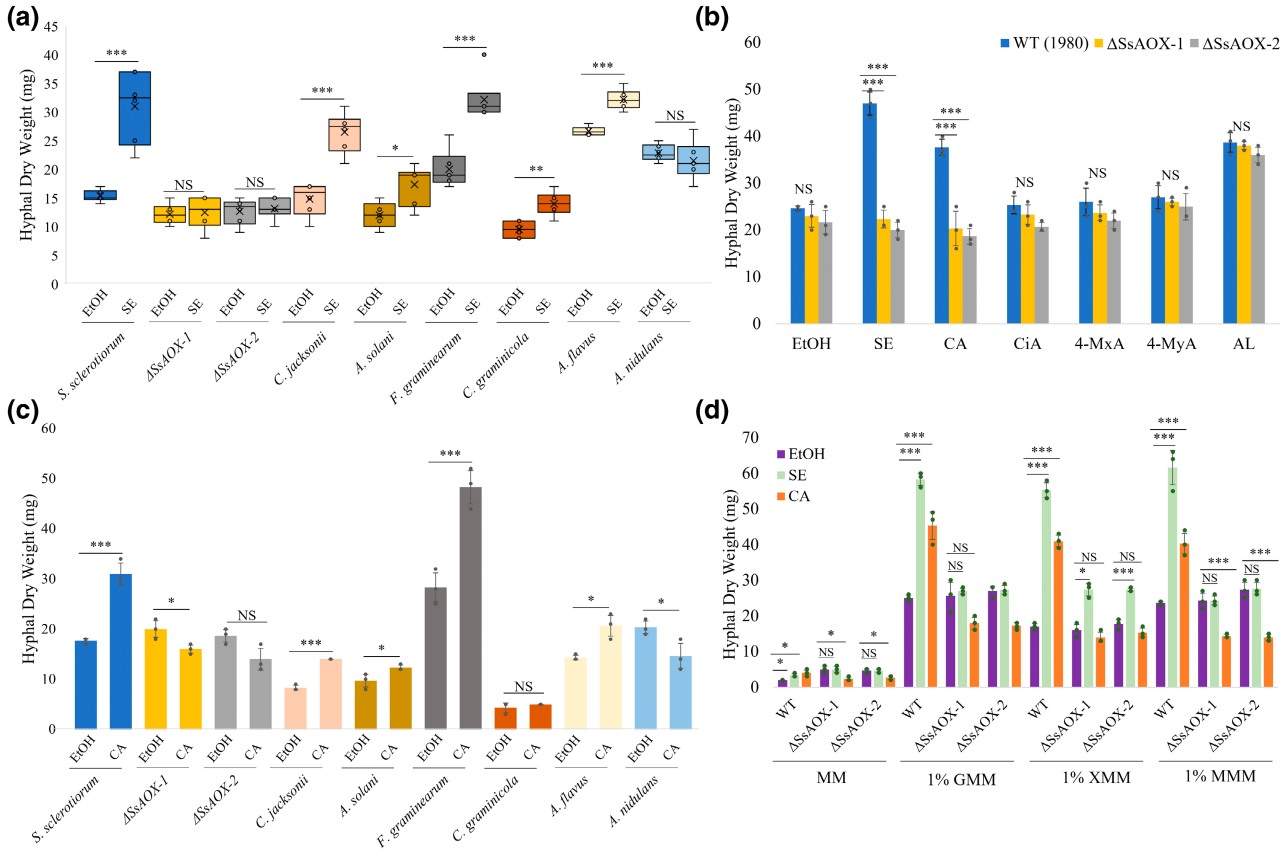

FIGURE 6 Fungal growth with the addition of soybean stem extract (SE) and aromatic alcohols. (a) Hyphal dry weight of wild type (WT), Δ*SsAOX* mutants, and other ascomycete fungi grown in 1% glucose minimal medium (GMM) with the addition of either 1% ethanol (control, EtOH) or 1% SE. (b) Hyphal dry weight of WT and Δ*SsAOX* mutants grown in 1% GMM with the addition of either 1% ethanol (control), 1% SE, coniferyl alcohol (CA), cinnamyl alcohol (CiA), 4-methoxybenzyl alcohol (4-MxA), 4-methylbenzyl alcohol (4-MyA), or alkali lignin (AL). All aromatic alcohols were dissolved in ethanol and added to a final concentration of 250 μM. AL was dissolved in ethanol and added to a final concentration of 50 μg/ml. (c) Growth induction of WT, Δ*SsAOX* mutants, and other ascomycete fungi grown in 1% GMM (250 μM CA) compared to the ethanol control. (d) Hyphal dry weight of WT and Δ*SsAOX* mutants grown in minimal medium (no carbon source, MM), 1% GMM, 1% xylose minimal medium (XMM), or 1% mannose minimal medium (MMM) with the addition of either 1% ethanol (control), 1% SE, or CA (250 μM). Colours in (a) and (c) indicate species/strain. Error bars in (b), (c), and (d) represent standard deviation. Cultures were grown for 3 days, except for *Colletotrichum graminicola*, which was grown for 4 days at room temperature on a shaker in the dark. Statistical analysis was conducted by comparing the results from each additive to the ethanol control using a Student's *t* test. $^{*}p < 0.05$, $^{**}p < 0.01$, $^{***}p < 0.001$.

with either ethanol or SE. SE addition amplified growth in C+N+ and C−N+ media, but no growth induction was observed when the samples were grown in media lacking nitrogen, suggesting that SE components other than nitrogen are enabling the growth of the WT (Figure S7). This is in accordance with previous data on the *AOX* orthologue in *P. fulva*, whose expression was found to be induced in carbon-poor, nitrogen-rich media (Segers et al., 2001). Further evidence of the importance of *SsAOX* in metabolism can be seen in the transcriptomic responses of the WT and mutant strains when grown in 1% GMM containing SE. A Kyoto Encyclopaedia of Genes and Genomes enrichment analysis of differentially expressed genes revealed a significant up-regulation of genes associated with primary carbon and amino acid metabolism in the WT when compared to the mutant in the presence of SE (Figure S8; Table S6).

To confirm that the SE growth phenotype observed in *S. sclerotiorum* extrapolates to other AOX-containing fungal species, ascomycetes spanning Leotiomycetes (*Clarireedia jacksonii*), Dothideomycetes (*Alternaria solani*), Sordariomycetes (*Colletotrichum graminicola*), and Eurotiomycetes (*A. flavus*, *Aspergillus nidulans*) were assessed. The addition of SE induced growth in all species with the exception of *A. nidulans* (Figure 6a). This may be related to the ecological niche of *A. nidulans*, as it is the only species among those tested that is not known to infect plants, or may be related to the insertion event seen in the *A. nidulans* copy of *AOX*, thus affecting its function (Figure S9). As previously mentioned, AOX appears to have a low tolerance for mutation as it is structurally conserved in both size and sequence across Pezizomycotina and computational modelling of multiple AOX orthologues suggests that the *A. nidulans* copy of AOX may have a unique alpha-helix in the C-terminus of the protein that could interfere with enzymatic activity or subcellular localization (Figure S9).

As a secondary validation of SsAOX's importance in the degradation/metabolism of plant tissue, WT and Δ*SsAOX* strains were inoculated on autoclaved carrots and allowed to colonize for several weeks. While there was no apparent defect in sclerotial formation when grown on PDA, the mass of sclerotia produced by Δ*SsAOX* during colonization of autoclaved carrot was significantly reduced when compared to WT (Figure S10). As no role for SsAOX in sclerotia production has been observed, this defect is probably due to a reduced capacity by the mutant strains to metabolize dead plant tissue.

2.5 | AOX regulates the *S. sclerotiorum* response to specific monolignols

Early theories of AOX activity from filamentous fungi focus on a role in methanol utilization, which mirrors the role of AOX in yeast such as *P. pastoris* (Segers et al., 2001). As pectin is heavily esterified, pectin methylesterases secreted by fungi probably lead to methanol release during infection and the role of a secreted methanol oxidase in methylotrophy has been demonstrated in the basidiomycete cacao pathogen *Moniliophthora perniciosa* (de Oliveira et al., 2012). Despite this, *SsAOX* appears transcriptionally decoupled from most members of the methanol metabolic pathway, all of which have been characterized in yeast and are known to be methanol-inducible (Figure S11a) (Yurimoto et al., 2011). This includes the *S. sclerotiorum* formaldehyde dehydrogenase (*SsFdh1*), which has been shown to be transcriptionally regulated by formaldehyde, the product of methanol oxidation, and does not increase in expression with *SsAOX* during infection (Figure S11a) (Zhu et al., 2019). Additionally, WT and Δ*SsAOX* mutants grew similarly in minimal media supplemented with glucose, pectin, or methanol, with neither capable of growing with methanol as a sole carbon source (Figure S11b).

While the AOX orthologue from *P. fulva* (79.8% identity to SsAOX) has limited enzymatic activity against methanol, previous research on the role of AOX in *A. terreus* (82.1% identity to SsAOX) suggests that the primary substrates of AOX from filamentous ascomycetes are aromatic alcohols (Chakraborty et al., 2014). To assess the potential role of SsAOX in metabolizing aromatic alcohols, WT and Δ*SsAOX* strains were grown in 1% GMM amended with various aromatic alcohols (Figure 6b). Cinnamyl alcohol, 4-methoxybenzyl alcohol, and 4-methylbenzyl alcohol induced slight growth in both WT and Δ*SsAOX*, but distinct divergence between the strains was seen when grown on coniferyl alcohol (CA), in which growth was strongly induced in the WT and slightly suppressed in Δ*SsAOX*. CA is one of the three primary monolignols used in the production of plant structural lignin, so the strains were additionally grown in media amended with alkali lignin, a polymer of lignin extracted from wood pulp. As both strains grew similarly in response to alkali lignin, it is likely that CA is not released upon *S. sclerotiorum* degradation of lignin (Figure 6b). To confirm that the growth induction phenotype of CA seen in the WT extrapolates beyond *S. sclerotiorum*, the previously described panel of fungi were tested on media amended with CA (Figure 6c). A growth induction similar to that of SE treatment was observed.

As the growth induction phenotypes observed in SsAOX suggest a clear role in metabolism, it was considered whether the carbon source present in media may play a role in its activity. To evaluate this, WT and Δ*SsAOX* were grown in minimal media containing glucose (GMM), xylose (XMM), mannose (MMM), or no carbon (MM) and were grown with the addition of SE, CA, or ethanol as a control. Broadly, the growth induction phenotypes observed in GMM were maintained, independent of the carbon source (Figure 6d). As it was initially theorized that SsAOX metabolizes aromatic alcohols as a carbon source, robust growth was expected from WT grown in MM with SE and CA as the sole carbon source. While a similar growth induction to other media types was observed when compared to ethanol, only a very modest increase in total hyphal mass (<3 mg) was observed from these additives as opposed to the significant mass increase seen in other media (more than about 30 mg) (Figure 6d). This suggests that SsAOX may be acting synergistically with other biochemical pathways to facilitate carbon utilization.

Broadly, AOXs interact with their substrate by oxidizing an alcohol group to their cognate aldehyde, which in the case of SsAOX would be the conversion of CA to coniferaldehye (CAld). To assess this possibility, WT and Δ*SsAOX-1* were grown in GMM supplemented with either ethanol or CA and then subjected to LC–MS

(Figure S12). As expected, a greater accumulation of CAld was detected in WT *S. sclerotiorum* than in the mutant strain, suggesting that CA is a possible substrate of SsAOX.

3 | DISCUSSION

Fungal AOXs have traditionally been discussed for the critical role that they play in plant–fungal interactions, both as drivers of methylotrophy in the phyllosphere and through the facilitation of lignin degradation by basidiomycete wood rot fungi (Hernández-Ortega et al., 2012; Yurimoto et al., 2011). Interestingly, these enzymes oxidize alcohols to generate cognate aldehydes and H_2O_2, either of which may be useful or detrimental to the fungus. In the case of methylotrophic yeast, formaldehyde is produced by AOX and then broken down as a carbon source, whereas in the case of wood rot fungi, the oxidation of *p*-methoxybenzyl alcohol to *p*-anisaldehyde is a means to produce prodigious amounts of H_2O_2 to drive extracellular peroxidase activity (Hernández-Ortega et al., 2012; Yurimoto et al., 2011). In this study, we identified a specific AOX orthologue that appears to have a function distinct from those previously described in fungi, with a wide distribution throughout the ascomycete subphylum Pezizomycotina.

3.1 | AOX gene loss is associated with carbon acquisition

Genomic evidence suggests that within Pezizomycotina, gene loss, rather than gene gain, is associated with the transition by some fungal clades from plant saprotrophy/pathogenicity to other ecological niches (Sanchez-Rodríguez et al., 2010). Our analysis suggests a similar phenomenon for *AOX*, given that the last common ancestor of Pezizomycotina probably contained an orthologue of *AOX*, and gene loss is observed in species that have transitioned away from plant material as a primary carbon source. The most striking example of this can be seen in the genomes of obligate animal pathogenic Pezizomycotina species, all of which have lost *AOX* (Table S4).

More broadly, *AOX* gene loss is consistently associated with some transition in ecological niche, be it animal pathogenicity, plant biotrophy/endophytism, growth on faecal matter, or lichenization (Figure 2b). Surprisingly, we also observed independent gene loss events in opportunistic animal pathogens, which are typically environmental saprophytes that might have a use for AOX in consuming plant carbohydrates (Lowe & Howlett, 2012). By analogy, a comparative genomic analysis of opportunistically pathogenic clinical isolates and plant isolates of *Fonsecaea* spp. revealed that genes that encode enzymes involved in phenolic degradation are enriched in plant isolates versus clinical isolates; this suggests that clinical isolates may be undergoing a shift away from reliance on plant material (Vicente et al., 2017). Such a relationship between opportunistic pathogenicity and plasticity in responding to novel environments has been hypothesized (Gostinčar et al., 2018). In summary, *AOX* orthologues are highly conserved in length, sequence, structure, and enzyme activity across large evolutionary distances (Figure 1; Figure S3), and gene loss of *AOX* in opportunistic fungal pathogens aligns with a shift in ecological niche away from reliance on plant tissue.

Comparative transcriptomics from a range of pathosystems have revealed that many virulence factors are only expressed in specific hosts/environments (Petre et al., 2020). To assess the expression of AOX among ascomycete plant pathogens, we analysed transcriptomic data sets from a diverse range of pathogens, including Eurotiomycetes, Sordariomycetes, Leotiomycetes, and Dothideomycetes, across a diversity of hosts, including angiosperms, gymnosperms, and bryophytes. Broadly, AOX orthologues appear to be highly up-regulated in all of these pathosystems, typically with increasing expression over the course of infection. The only exceptions to this are during infection of tomato fruit and wheat seeds, both of which have a much more lignified exterior, suggesting that AOX may play a role in colonization of lignified plant tissue. This explanation is confounded somewhat as *B. cinerea* expresses *AOX* during infection of the nonvascular, lignin-deficient *P. patens*, but *P. patens* probably produces the monomeric components of lignin, if not the structural component itself (Martínez-Cortés et al., 2021).

3.2 | SsAOX plays an important role in plant pathogenicity and the response to monolignols

To assess the role of *AOX* in development and virulence, we deleted *SsAOX* in *S. sclerotiorum*. This predominantly necrotrophic pathogen demonstrates a remarkably wide host range, including economically important dicotyledonous plants (Kabbage et al., 2015). We observed that Δ*SsAOX* mutants were less virulent to both detached soybean leaves and whole plants and demonstrated a surprising defect in colonization of stem vascular tissue. Metabolomic profiling of WT and Δ*SsAOX* infection suggests that the mutant probably macerates host tissue to a lesser degree than the WT during infection. We postulated that Δ*SsAOX* mutation affects how the fungus utilizes or tolerates some plant metabolites. Indeed, when the mutant and WT were grown in media containing soybean SE, we observed significant growth in WT *S. sclerotiorum* and a number of other *AOX*-containing species, but not Δ*SsAOX*. This validates previous studies on the tomato leaf mould pathogen *P. fulvum*, in which *AOX* knockouts were significantly less virulent on tomato leaves, and the oat pathogen *Cochliobolus victoriae*, in which *AOX* overexpression strains demonstrated increased growth compared to controls (Segers et al., 2001; Zhao et al., 2006).

There is much to learn about the substrate of choice for this ascomycete AOX; only a small number of short-chain alcohols have been tested as substrate, such that methanol was assumed to be the primary substrate despite limited enzymatic activity (Holzmann et al., 2002; Isobe et al., 2007; Segers et al., 2001). To the best of our knowledge, no study has yet demonstrated a capacity for filamentous ascomycetes to utilize methanol. Additionally, *S. sclerotiorum* cannot use methanol as a carbon source, and the enzymatic

machinery required for methylotrophy is enzymatically decoupled from *AOX* expression in planta (Figure S10). Intriguingly, an AOX study in *A. terreus* showed that this enzyme has minimal activity on short-chain alcohols and is much more efficient in oxidizing aromatic (aryl-) alcohols, which could be its primary target (Chakraborty et al., 2014). In this study, a clear deviation in growth was observed between Δ*SsAOX* and WT *S. sclerotiorum* in response to media amended with CA, suggesting that this monolignol may be a substrate of SsAOX. This possibility is intriguing as CA is a base component of lignin and therefore enriched in lignified plant material, is stored in plant vacuoles, and is probably released in response to pathogen infection (Dima et al., 2015).

The role of SsAOX in aryl-alcohol oxidation presents an interesting question, as aldehydes are often inhibitory to fungal growth (Battinelli et al., 2006; Kishimoto et al., 2008). The simplest explanation is that the conversion of aryl-alcohols to aryl-aldehydes is simply the first step in a carbon utilization or detoxification pathway (Yurimoto et al., 2011). The data presented in this study suggest that *SsAOX* may be acting directly on aromatic alcohols released from plant tissue, but previous work on the *SsAOX* orthologue in *A. terreus* suggested that the fungus may convert a wider range of aromatic compounds to aromatic alcohols (possibly through cytochrome P450 activity), which are then metabolized through AOX activity (Chakraborty et al., 2014). Interestingly, *S. sclerotiorum* encodes and expresses a vanillyl-alcohol oxidase (Sscle02g021040) during infection, the orthologue of which is broadly conserved in Pezizomycotina and has been shown in *Penicillium simplicissimum* to be capable of converting a range of phenolic compounds to aromatic alcohols (Gygli et al., 2018). Synergistic activity between peroxisomes and mitochondria to facilitate fatty acid biosynthesis has been studied in animal systems and it is additionally possible that AOX is also driving similar activity in fungi (Wanders et al., 2016). Such activity may help to explain why the addition of SE led to such dramatic growth for the WT in media containing carbon when compared to media without added carbon. Finally, it is possible that SsAOX oxidation of an alcohol substrate would simply act as a mechanism to generate the H_2O_2 that is produced as a result of alcohol oxidation, as is seen in the secreted aryl-alcohol oxidase of *Pleurotus* spp. (Hernández-Ortega et al., 2012). This H_2O_2 could act as a cofactor in another enzymatic reaction or as an important signalling molecule in fungi, leading to the activation of other plant-specific processes. Importantly, our data suggest that AOX orthologues play an important role in the metabolism of plant material across a number of ascomycetes, but does not imply its absolute necessity. Within our data set, a number of fungi that interact with plant material, at least at some point during their life cycle, including *Fusarium proliferatum*, *Cordyceps militaris*, and *Aspergillus fumigatus*, were found to have lost AOX, implying that some AOX loss may be driven by these fungi developing novel mechanisms to interact with monolignols. Such a possibility is intriguing as *F. proliferatum* is known for its capacity to degrade lignin and will be the focus of future research (Anderson et al., 2005). Overall, this study provides evidence for the preservation and utilization of a structurally conserved AOX during plant colonization by a wide group of fungi. Although the precise mechanics and substrate range of AOX will be the goal of further investigation, the importance in virulence has been established in multiple pathosystems and may be an important driver of plant–fungal interactions across a range of trophic lifestyles.

4 | EXPERIMENTAL PROCEDURES

4.1 | Plant and fungal growth

All plant material was maintained in the greenhouse or growth chamber at 24 ± 2°C with a 16-h light/8-h dark photoperiod cycle. Plants were watered daily and supplemented with fertilizer (Miracle-Gro) every week.

All fungal cultures were maintained on PDA plates or PDA supplemented with 50 μg/ml hygromycin in the case of knockout strains. Liquid cultures were maintained in minimal medium (MM) supplemented with either 1% glucose (GMM), 1% xylose (XMM), or 1% mannose (MMM) and grown at room temperature (Shimizu & Keller, 2001). Plates were grown with an approximate 16-h light/8-h dark photoperiod cycle and liquid cultures were wrapped in foil to maintain full darkness. GMM cultures were inoculated from PDA plugs of actively growing hyphae.

Carrot cultures were prepared by autoclaving 25 g of chopped carrots with 10 ml of water in 250-ml Erlenmeyer flasks for 20 min. Three agar plugs of actively growing hyphae were inoculated in each flask and allowed to grow for 6 weeks in the dark at room temperature. Carrot material was separated from sclerotia using a metal soil sieve and sclerotia were sterilized for 1 min in 10% bleach followed by 1 min in 70% ethanol, and then rinsed three times in sterile water for 1 min. Sclerotia were dried for 2 h in a laminar flow hood prior to being weighed.

4.2 | Growth induction/suppression assays

All growth induction/suppression assays were conducted in six-well plates (Dot Scientific: 229506) containing 10 ml of autoclaved GMM per well. Each well was supplemented with either 100 μl ethanol, 100 μl soybean SE, or 100 μl of tested compounds dissolved in ethanol at a concentration of 25 mM (final concentration 250 μM). The top 2 mm of actively growing hyphae were excised from 5-mm agar plugs and were used to inoculate wells. Fungi were grown at room temperature for 3–6 days (dependent on species) in the dark prior to collection. Hyphae were collected from liquid culture and dried overnight in an oven at 65°C in tared weigh boats prior to weighing. Three to six biological replicates were used for each sample and *p* values were generated from a Student's *t* test.

Soybean SE was collected from 5- to 6-week-old soybean stems. Briefly, soybean stem segments between the first and third trifoliate were cut into 2.5–5-cm segments and frozen in liquid nitrogen. Segments were roughly ground with a mortar and pestle and about

12 g of stem material was placed in a 50-ml Falcon tube along with 100% ethanol to the 50 ml mark. Tubes were placed at −80°C overnight prior to filtering through Miracloth. SE was stored at −80°C.

All assays were conducted with a WT (1980) control and two independent *SsAOX* knockout strains. A Student's *t* test was used to compare the growth of the two strains for each experiment, and only a single strain is presented in figures for assays in which the difference between the two strains was statistically insignificant.

4.3 | Plant disease assays

4.3.1 | Whole plant disease assays

Soybean plants were grown for 5 weeks prior to being infected with WT (1980) or mutant *S. sclerotiorum* by petiole inoculation as previously described (Ranjan et al., 2019). Stem lesions were measured every 24 h for 6 days.

4.3.2 | Detached leaf assays

Leaves were taken from the first trifoliate of 5-week-old soybean plants and placed in Petri dishes containing two layers of filter paper and 7 ml of sterile water. Leaves were inoculated near the centre with agar plugs of actively growing WT (1980) or mutant *S. sclerotiorum*. Petri dishes were then wrapped in Parafilm and placed on the bench top to be photographed every 24 h.

Lesions were quantified using ImageJ (Schneider et al., 2012). Trypan blue staining and leaf clearing were performed in accordance with the protocol described in Fernández-Bautista et al. (2016).

All assays were conducted with a WT (1980) control and two independent *SsAOX* knockout strains. A Student's *t* test was used to compare the growth of the two strains for each experiment, and only a single strain is presented in figures for assays in which the difference between the two strains was statistically insignificant.

4.4 | AOX phylogeny and protein modelling

S. sclerotiorum AOX (*SsAOX*; SS1G_00840 and Sscle03g024060; XM_001598701.1) was used as the query in a Protein BLAST (blastp) targeting the RefSeq protein database filtered for species within Ascomycota (O'Leary et al., 2016). To confirm that species lacking an AOX blastp hit were properly queryable, all species were subject to a blastp search against the actin protein from *Trichoderma reesei* (XP_006961104.1) and species with no hits were removed from the analysis. To identify orthologues and exclude homologous proteins from related families, only blastp hits of >60% amino acid identity and >70% coverage were counted as true AOX orthologues. This threshold was set based on a clear drop-off in sequence homology below 60% amino acid identity and the apparent interrelatedness of protein hits below this level (Figure S13). The presence/absence of AOX was determined by comparing species with a positive blastp hit to the overall list of Ascomycete fungi in RefSeq.

Phylogenic relationships were characterized with the NCBI Taxonomy Browser and the Joint Genome Institute Mycocosm Database (Grigoriev et al., 2014; Schoch et al., 2020). Gene intron counts were collected from the Ensembl Genome Database (Howe et al., 2020).

Computational modelling of protein tertiary structures was performed with Phyre2 (Kelley et al., 2016). Protein structural alignments were performed using Partial Order Structure Alignment (Li et al., 2014).

4.5 | Fungal transformation

Gene knockouts were generated in *S. sclerotiorum* using a novel CRISPR/Cas9 approach in combination with a modified variation of the Rollins (2003) protocol. Split markers targeting *SsAOX* were generated by amplifying 500–600-bp regions upstream (SsAOX-LF-F and SsAOX LF-R) and downstream (SsAOX-RF-F and SsAOX-RF-R) of *SsAOX* using PCR. These amplicons were designed to contain 20-bp sequences with homology to the 5′ and 3′ regions, respectively, of the hygromycin resistance cassette (*HygR*; 1.8 kb) found in pCRISPR-Cas9-TrpC-Hyg (Li et al., 2018). The *HygR* cassette including promoter and terminator was amplified using the primers HygDet F and HygDet R. The two flanking regions and *HygR* were connected through fusion PCR as described in Szewczyk et al. (2006) for a product of about 3 kb (Szewczyk et al., 2006). Split markers were generated from this product as described in Catlett et al. (2003), using primers internal to *HygR* (Hyg Split F and Hyg Split R) in conjunction with SsAOX-RF-F and SsAOX-RF-R, yielding two fragments with an overlapping region of about 400 bp (Catlett et al., 2003).

Two small guide RNAs (sgRNAs) targeting *SsAOX* were designed using the E-CRISP Design Tool (http://www.e-crisp.org/E-CRISP/index.html) and generated using the GenCrispr sgRNA Screening Kit (L00689; Genscript Biotech Corp.). These sgRNAs were diluted to a concentration of 4 μM. Alt-R S.p. Cas9 nuclease 3NLS (1081058; IDT) was diluted to a concentration of 4 μM and combined with sgRNA at a 1.2:1 ratio (3.6 μl of sgRNA to 3 μl of Cas9 protein) and incubated at room temperature for at least 5 min to assemble the ribonucleoprotein complex. Ribonucleoprotein complexes were combined with 1 μg of each split marker and transfected into *S. sclerotiorum* protoplasts using the polyethylene glycol transformation protocol described in Rollins (2003).

Transformants capable of surviving on PDA containing 50 μg/ml hygromycin were subjected to five rounds of hyphal tipping before undergoing DNA extraction to confirm the replacement of *SsAOX* with the *HygR* marker. *SsAOX* detection primers (SsAOX Det F and SsAOX Det R) were used to confirm deletion, and primers targeting *Histone 3* (H3 F and H3 R) were used as a control (Figure S14; Table S7). The transformants used in this study were selected from distinct protoplast populations (i.e., protoplasts transfected in

separate tubes and selected on distinct plates) to ensure independent transformation events.

4.6 | DNA extraction

Fungal DNA was extracted using a modified CTAB method. Briefly, fungal hyphae were grown in potato dextrose broth for 3 days at room temperature while shaking at 100 rpm. Samples were collected and rinsed briefly in sterile water before being frozen in liquid nitrogen and ground with an autoclaved mortar and pestle. Two-millilitre microcentrifuge tubes were filled to 500 µl with powdered frozen hyphae and stored at −80°C. Seven hundred microlitres of 2% CTAB extraction buffer prewarmed to 65°C was added to each tube, followed by 7 µl of 2-mercaptoethanol. Samples were vortexed and placed in a 65°C incubator for 30 min, with a brief vortex at the halfway point. Four hundred microlitres of chloroform:isoamyl alcohol (24:1 vol/vol) was added to each sample, and samples were briefly vortexed and centrifuged at 16,000 × *g* for 5 min to separate phases. Approximately 600 µl was taken from the top phase of each sample and each sample was subjected to isopropanol precipitation, followed by two cold 75% ethanol washes prior to being dried and eluted in nuclease-free water.

4.7 | Metabolite estimation and analysis

Six-week-old soybean plants (Williams 82) were petiole inoculated as described above. Four stems (3 cm) for each treatment per biological replicate were harvested 96 h postinoculation and noninoculated stems were used as a control. Samples were flash frozen in liquid nitrogen and kept at −80°C until used. GC–MS analysis was performed by West Coast Metabolomics (University of California). Detailed methods of metabolite derivatization, separation, and detection are described in Fiehn (2016). Briefly, samples were injected (0.5 µl, splitless injection) into a Pegasus IV GC (Leco Corp.) equipped with a 30 m × 0.25 mm i.d. fused-silica capillary column bound with 0.25 µm Rtx-5Sil MS stationary phase (Restek Corp.). The injector temperature was 50°C ramped to 250°C by 12°C/s. A helium mobile phase was applied at a flow rate of 1 ml/min. Column temperature was 50°C for 1 min, ramped to 330°C by 20°C/min, and held constant for 5 min. The column effluent was introduced into the ion source of a Pegasus IV TOF MS (Leco Corp.) with transfer line temperature set to 230°C and ion source set to 250°C. Ions were generated with an ionization energy of −70 eV and 1800 V. Masses (80–500 *m*/*z*) were acquired at a rate of 17 spectra per second. ChromaTOF v. 2.32 software (Leco Corp.) was used for automatic peak detection and deconvolution using a peak width of 3 s. Peaks with signal:noise below 5:1 were rejected. Metabolites were quantified by peak height for the quantification ion. Metabolites were annotated with the BinBase v. 2.0 algorithm (Skogerson et al., 2011). Statistical and principal component analyses were conducted in MetaboAnalyst v 3.0 using default values (Xia et al., 2015). Metabolite peak heights were subject to a Student's *t* test and those with $p < 0.05$ were considered differentially accumulated.

4.8 | RNA-Seq and RNA-Seq analysis from diverse pathosystems

WT (1980) and mutant strains were grown in 1% GMM for 3 days before cultures were moved to fresh medium containing 1% soybean SE and allowed to grow for 4 h prior to flash freezing in liquid nitrogen. RNA was extracted with a Maxwell RSC Plant RNA Kit (AS1500). Illumina raw read data quality was verified with FastQC. The *S. sclerotiorum* genome and gene annotations were collected from the Ensembl Fungi (Howe et al., 2020). Raw sequence reads were mapped to both genomes using the Subjunc aligner from Subread (Liao et al., 2013). Alignments were compared to the gene annotation GFF file of *S. sclerotiorum*, sclerotinia_sclerotiorum_2_transcripts.gtf (Amselem et al., 2011), and raw counts for each gene were generated using the feature Counts tool from Subread. The raw counts data were normalized with the DESeq normalization method using the DESeq2 package (Love et al., 2014). The normalized gene counts were transformed to $\log_2$ scale using the voom method from the R Limma package and then used to generate differential expression ($\log_2$(fold change)) values (Law et al., 2014; Ritchie et al., 2015).

Differential gene expression values were additionally culled from data sets published in other pathosystems: *S. sclerotiorum*–soybean, Westrick et al. (2019); *S. sclerotiorum*–chickpea, Mwape et al. (2021); *B. cinerea*–tomato, Petrasch et al. (2019); *B. cinerea*–*P. patens*, Reboledo et al. (2021); *A. flavus*–peanut, Wang et al. (2016); *F. oxysporum*–cucumber, Huang et al. (2019); *F. graminearum*–wheat, Puri et al. (2016); and *D. septosporum*–pine, Bradshaw et al. (2016. For each pathosystem, the fungal orthologue of *SsAOX* was identified through blastp and the fold change values comparing timepoints during infection to an in vitro control were pulled from supplementary data.

4.9 | Metabolite extraction

Thin (2-mm) agar plugs of WT (1980) and Δ*SsAOX-1* were placed in 10 ml of 1% GMM supplemented with either 1% ethanol (100 µl) or CA to a final concentration of 250 µM (100 µl of 25 mM CA in ethanol). Cultures were grown for 3 days in the dark on a shaker at 90 rpm, before being lyophilized for 24 h, crushed in mortar and pestle, and normalized to the lowest sample weight. Six independent cultures were combined for each treatment. Lyophilized hyphae were then placed in 25 ml of ethanol overnight at room temperature to extract compounds of interest, followed by filtering through sterile 0.45-µm filters. Each extract was evaporated and dried weight of extracts were measured. Crude extracts were suspended with methanol at a final concentration of 1 µg/ml. Each sample was analysed by ultrahigh-performance liquid chromatography high-resolution mass spectrometry (UHPLC-HRMS).

4.10 | UHPLC-HRMS analysis

UHPLC-HRMS was performed on a Thermo Scientific Vanquish UHPLC system connected to a Thermo Scientific Q Exactive Hybrid Quadrupole-Orbitrap mass spectrometer operated in negative ionization mode. An Agilent Zorbax Eclipse XDB-C18 column (2.1 × 150 mm, 1.8 μm) was used with acetonitrile (0.1% formic acid) and water (0.1% formic acid) as solvents at a flow rate of 0.2 ml/min. The screening gradient method for the extracts was as follows: starting at 10% organic for 5 min, followed by a linear increase to 90% organic over 20 min, another linear increase to 98% organic for 2 min, holding at 98% organic for 5 min, decreasing back to 10% organic for 3 min, and holding at 10% organic for the final 2 min, for a total of 37 min. A quantity of 10 μl of each sample was injected into the system for the analysis. CAld from the extracts was identified by injecting standard CAld to the same method. The fold accumulation was calculated based on the intensity of CAld from each extract.

ACKNOWLEDGEMENTS

We would like to express our gratitude to Grant Nickles for the generation of the phylogenetic tree used in this study. We would like to thank the USDA National Institute of Food and Agriculture (2021-67011-35151 to N.M.W.), the USDA ARS National Sclerotinia Initiative (58-3060-8-023 to M.K. and D.S.), and USDA Hatch (Wis04031 to M.K.) for supporting this research.

CONFLICT OF INTEREST

The authors declare no conflict of interest.

DATA AVAILABILITY STATEMENT

A majority of raw data is included in supplemental tables and RNA-Seq data is publicly available in the NCBI Gene Expression Omnibus (GEO) at https://www.ncbi.nlm.nih.gov/geo/ under accession number GSE212269.

ORCID

Nathaniel M. Westrick https://orcid.org/0000-0002-0282-675X
Nancy P. Keller https://orcid.org/0000-0002-4386-9473

REFERENCES

Amselem, J., Cuomo, C.A., vanKan, J.A.L., Viaud, M., Benito, E.P., Couloux, A. et al. (2011) Genomic analysis of the necrotrophic fungal pathogens *Sclerotinia sclerotiorum* and *Botrytis cinerea*. *PLoS Genetics*, 7, e1002230.

Anderson, A.J., Kwon, S.-I., Carnicero, A. & Falcón, M.A. (2005) Two isolates of *Fusarium proliferatum* from different habitats and global locations have similar abilities to degrade lignin. *FEMS Microbiology Letters*, 249, 149–155.

Andrews, J., Adams, S.R., Burton, K.S. & Evered, C.E. (2002) Subcellular localization of peroxidase in tomato fruit skin and the possible implications for the regulation of fruit growth. *Journal of Experimental Botany*, 53, 2185–2191.

Asthir, B., Kaur, S., Spoor, W. & Roitsch, T. (2010) Spatial and temporal dynamics of peroxidase and amine oxidase activity is linked to polyamines and lignin in wheat grains. *Biologia Plantarum*, 54, 525–529.

Battinelli, L., Daniele, C., Cristiani, M., Bisignano, G., Saija, A. & Mazzanti, G. (2006) In vitro antifungal and anti-elastase activity of some aliphatic aldehydes from *Olea europaea* L. fruit. *Phytomedicine*, 13, 558–563.

Becker, M., Becker, Y., Green, K. & Scott, B. (2016) The endophytic symbiont *Epichloë festucae* establishes an epiphyllous net on the surface of *Lolium perenne* leaves by development of an expressorium, an appressorium-like leaf exit structure. *New Phytologist*, 211, 240–254.

Bradshaw, R.E., Guo, Y., Sim, A.D., Kabir, M.S., Chettri, P., Ozturk, I.K. et al. (2016) Genome-wide gene expression dynamics of the fungal pathogen *Dothistroma septosporum* throughout its infection cycle of the gymnosperm host *Pinus radiata*. *Molecular Plant Pathology*, 17, 210–224.

Carmel, L., Rogozin, I.B., Wolf, Y.I. & Koonin, E.V. (2007) Evolutionarily conserved genes preferentially accumulate introns. *Genome Research*, 17, 1045–1050.

Catlett, N.L., Lee, B.N., Yoder, O.C. & Turgeon, B.G. (2003) Split-marker recombination for efficient targeted deletion of fungal genes. *Fungal Genetics Reports*, 50, 9–11.

Chakraborty, M., Goel, M., Chinnadayyala, S.R., Dahiya, U.R., Ghosh, S.S. & Goswami, P. (2014) Molecular characterization and expression of a novel alcohol oxidase from *Aspergillus terreus* MTCC6324. *PLoS One*, 9, e95368.

Cregg, J.M., Madden, K.R., Barringer, K.J., Thill, G.P. & Stillman, C.A. (1989) Functional characterization of the two alcohol oxidase genes from the yeast *Pichia pastoris*. *Molecular and Cellular Biology*, 9, 1316–1323.

Csuros, M., Rogozin, I.B. & Koonin, E.V. (2011) A detailed history of intron-rich eukaryotic ancestors inferred from a global survey of 100 complete genomes. *PLoS Computational Biology*, 7, e1002150.

Dima, O., Morreel, K., Vanholme, B., Kim, H., Ralph, J. & Boerjan, W. (2015) Small glycosylated lignin oligomers are stored in *Arabidopsis* leaf vacuoles. *The Plant Cell*, 27, 695–710.

Fernández-Bautista, N., Domínguez-Núñez, J.A., Moreno, M.M.C. & Berrocal-Lobo, M. (2016) Plant tissue trypan blue staining during phytopathogen infection. *Bio-protocol*, 6, e2078.

Fiehn, O. (2016) Metabolomics by gas chromatography-mass spectrometry: combined targeted and untargeted profiling. *Current Protocols in Molecular Biology*, 114, 30.4.1–30.4.32.

Galperin, I., Javeed, A., Luig, H., Lochnit, G. & Rühl, M. (2016) An aryl-alcohol oxidase of *Pleurotus sapidus*: heterologous expression, characterization, and application in a 2-enzyme system. *Applied Microbiology and Biotechnology*, 100, 8021–8030.

Gazis, R., Kuo, A., Riley, R., LaButti, K., Lipzen, A., Lin, J. et al. (2016) The genome of *Xylona heveae* provides a window into fungal endophytism. *Fungal Biology*, 120, 26–42.

Gostinčar, C., Zajc, J., Lenassi, M., Plemenitaš, A., de Hoog, S., al-Hatmi, A.M.S. et al. (2018) Fungi between extremotolerance and opportunistic pathogenicity on humans. *Fungal Diversity*, 93, 195–213.

Grigoriev, I.V., Nikitin, R., Haridas, S., Kuo, A., Ohm, R., Otillar, R. et al. (2014) MycoCosm portal: gearing up for 1000 fungal genomes. *Nucleic Acids Research*, 42(D1), 699–704.

Gygli, G., de Vries, R.P. & van Berkel, W.J.H. (2018) On the origin of vanillyl alcohol oxidases. *Fungal Genetics and Biology*, 116, 24–32.

He, M. & Ding, N.Z. (2020) Plant unsaturated fatty acids: multiple roles in stress response. *Frontiers in Plant Science*, 11, 562785.

Hernández-Ortega, A., Ferreira, P. & Martínez, A.T. (2012) Fungal aryl-alcohol oxidase: a peroxide-producing flavoenzyme involved in lignin degradation. *Applied Microbiology and Biotechnology*, 93, 1395–1410.

Holzmann, K., Schreiner, E. & Schwab, H. (2002) A *Penicillium chrysogenum* gene (*Aox*) identified by specific induction upon shifting pH encodes for a protein which shows high homology to fungal alcohol oxidases. *Current Genetics*, 40, 339–344.

Howe, K.L., Contreras-Moreira, B., De Silva, N., Maslen, G., Akanni, W., Allen, J. et al. (2020) Ensembl genomes 2020 €°¡# enabling non-vertebrate genomic research. *Nucleic Acids Research*, 48(D1), D689–D695.

Huang, X.Q., Lu, X.-H., Sun, M.-H., Guo, R.-J., Van Diepeningen, A.D. & Li, S.-D. (2019) Transcriptome analysis of virulence-differentiated *Fusarium oxysporum* f. sp. *cucumerinum* isolates during cucumber colonisation reveals pathogenicity profiles. *BMC Genomics*, 20, 570.

Huisjes, E.H., de Hulster, E., van Dam, J.C., Pronk, J.T. & van Maris, A.J. (2012) Galacturonic acid inhibits the growth of *Saccharomyces cerevisiae* on galactose, xylose, arabinose. *Applied and Environmental Microbiology*, 78, 5052–5059.

Ibrahim, H.M.M., Kusch, S., Didelon, M. & Raffaele, S. (2021) Genome-wide alternative splicing profiling in the fungal plant pathogen *Sclerotinia sclerotiorum* during the colonization of diverse host families. *Molecular Plant Pathology*, 22, 31–47.

Isobe, K., Kato, A., Ogawa, J., Kataoka, M., Iwasaki, A., Hasegawa, J. et al. (2007) Characterization of alcohol oxidase from *Aspergillus ochraceus* AIU 031. *Journal of General and Applied Microbiology*, 53, 177–183.

Kabbage, M., Yarden, O. & Dickman, M.B. (2015) Pathogenic attributes of *Sclerotinia sclerotiorum*: switching from a biotrophic to necrotrophic lifestyle. *Plant Science*, 233, 53–60.

Kachroo, A., Fu, D.-Q., Havens, W., Navarre, D.R., Kachroo, P. & Ghabrial, S.A. (2008) An oleic acid-mediated pathway induces constitutive defense signaling and enhanced resistance to multiple pathogens in soybean. *Molecular Plant-Microbe Interactions*, 21, 564–575.

Kelley, L.A., Mezulis, S., Yates, C.M., Wass, M.N. & Sternberg, M.J. (2016) The Phyre2 web portal for protein modeling, prediction and analysis. *Nature Protocols*, 10, 845–858.

Kishimoto, K., Matsui, K., Ozawa, R. & Takabayashi, J. (2008) Direct fungicidal activities of C6-aldehydes are important constituents for defense responses in *Arabidopsis* against *Botrytis cinerea*. *Phytochemistry*, *69*, 2127–2132.

Kubicek, C.P., Starr, T.L. & Louise Glass, N. (2014) Plant cell wall–degrading enzymes and their secretion in plant-pathogenic fungi. *Annual Review of Phytopathology*, 52, 427–451.

Kupfer, D.M., Drabenstot, S.D., Buchanan, K.L., Lai, H., Zhu, H., Dyer, D.W. et al. (2004) Introns and splicing elements of five diverse fungi. *Eukaryotic Cell*, 3, 1088–1100.

Kusch, S., Larrouy, J., Ibrahim, H.M.M., Mounichetty, S., Gasset, N., Navaud, O. et al. (2021) Transcriptional response to host chemical cues underpins the expansion of host range in a fungal plant pathogen lineage. *ISME Journal*, 16, 138–148.

Law, C.W., Chen, Y., Shi, W. & Smyth, G.K. (2014) Voom: precision weights unlock linear model analysis tools for RNA-seq read counts. *Genome Biology*, 15, R29.

Lenk, M., Wenig, M., Bauer, K., Hug, F., Knappe, C., Lange, B. et al. (2019) Pipecolic acid is induced in barley upon infection and triggers immune responses associated with elevated nitric oxide accumulation. *Molecular Plant-Microbe Interactions*, 32, 1303–1313.

Li, J., Zhang, Y., Zhang, Y., Yu, P.L., Pan, H. & Rollins, J.A. (2018) Introduction of large sequence inserts by CRISPR-Cas9 to create pathogenicity mutants in the multinucleate filamentous pathogen *Sclerotinia sclerotiorum*. *mBio*, *9*, e00567-18.

Li, Z., Natarajan, P., Ye, Y., Hrabe, T. & Godzik, A. (2014) POSA: a user-driven, interactive multiple protein structure alignment server. *Nucleic Acids Research*, 42(W1), 240–245.

Liao, Y., Smyth, G.K. & Shi, W. (2013) The subread aligner: fast, accurate and scalable read mapping by seed-and-vote. *Nucleic Acids Research*, 41, e108.

Love, M.I., Huber, W. & Anders, S. (2014) Moderated estimation of fold change and dispersion for RNA-seq data with DESeq2. *Genome Biology*, 15, 550.

Lowe, R.G.T. & Howlett, B.J. (2012) Indifferent, affectionate, or deceitful: lifestyles and secretomes of fungi. *PLoS Pathogens*, 8, e1002515.

Lutzoni, F., Nowak, M.D., Alfaro, M.E., Reeb, V., Miadlikowska, J., Krug, M. et al. (2018) Contemporaneous radiations of fungi and plants linked to symbiosis. *Nature Communications*, 9, 5451.

Martínez-Cortés, T., Pomar, F. & Novo-Uzal, E. (2021) Evolutionary implications of a peroxidase with high affinity for cinnamyl alcohols from *Physcomitrium patens*, a non-vascular plant. *Plants*, 10, 1476.

Mwape, V.W., Mobegi, F.M., Regmi, R., Newman, T.E., Kamphuis, L.G. & Derbyshire, M.C. (2021) Analysis of differentially expressed *Sclerotinia sclerotiorum* genes during the interaction with moderately resistant and highly susceptible chickpea lines. *BMC Genomics*, 22, 333.

O'Leary, N.A., Wright, M.W., Brister, J.R., Ciufo, S., Haddad, D., McVeigh, R. et al. (2016) Reference sequence (RefSeq) database at NCBI: current status, taxonomic expansion, and functional annotation. *Nucleic Acids Research*, 44(D1), D733–d745.

de Oliveira, B.V., Teixeira, G.S., Reis, O., Barau, J.G., Teixeira, P.J.P.L., do Rio, M.C.S. et al. (2012) A potential role for an extracellular methanol oxidase secreted by *Moniliophthora perniciosa* in witches' broom disease in cacao. *Fungal Genetics and Biology*, 49, 922–932.

Petrasch, S., Silva, C.J., Mesquida-Pesci, S.D., Gallegos, K., van den Abeele, C., Papin, V. et al. (2019) Infection strategies deployed by *Botrytis cinerea*, *Fusarium acuminatum*, and *Rhizopus stolonifer* as a function of tomato fruit ripening stage. *Frontiers in Plant Science*, 10, 233.

Petre, B., Lorrain, C., Stukenbrock, E.H. & Duplessis, S. (2020) Host-specialized transcriptome of plant-associated organisms. *Current Opinion in Plant Biology*, 56, 81–88.

Puri, K.D., Yan, C., Leng, Y. & Zhong, S. (2016) RNA-seq revealed differences in transcriptomes between 3ADON and 15ADON populations of *Fusarium graminearum* in vitro and in planta. *PLoS One*, 11, e0163803.

Ranjan, A., Westrick, N.M., Jain, S., Piotrowski, J.S., Ranjan, M., Kessens, R. et al. (2019) Resistance against *Sclerotinia sclerotiorum* in soybean involves a reprogramming of the phenylpropanoid pathway and up-regulation of antifungal activity targeting ergosterol biosynthesis. *Plant Biotechnology Journal*, 17, 1567–1581.

Reboledo, G., Agorio, A., Vignale, L., Batista-García, R.A. & Ponce De León, I. (2021) *Botrytis cinerea* transcriptome during the infection process of the bryophyte *Physcomitrium patens* and angiosperms. *Journal of Fungi*, 7, 11.

Ritchie, M.E., Phipson, B., Wu, D., Hu, Y., Law, C.W., Shi, W. et al. (2015) Limma powers differential expression analyses for RNA-sequencing and microarray studies. *Nucleic Acids Research*, 43, e47.

Rollins, J. (2003) The *Sclerotinia sclerotiorum Pac1* gene is required for sclerotial development and virulence. *Molecular Plant-Microbe Interactions*, 16, 785–795.

Sanchez-Rodríguez, A., Martens, C., Engelen, K., Van de Peer, Y. & Marchal, K. (2010) The potential for pathogenicity was present in the ancestor of the ascomycete subphylum Pezizomycotina. *BMC Evolutionary Biology*, 10, 318.

Schneider, C.A., Rasband, W.S. & Eliceiri, K.W. (2012) NIH image to ImageJ: 25 years of image analysis. *Nature Methods*, *9*, 671–675.

Schoch, C.L., Ciufo, S., Domrachev, M., Hotton, C.L., Kannan, S., Khovanskaya, R. et al. (2020) NCBI taxonomy: a comprehensive update on curation, resources and tools. *Database*, 2020, 1–21.

Sederoff, R.R., MacKay, J.J., Ralph, J. & Hatfield, R.D. (1999) Unexpected variation in lignin. *Current Opinion in Plant Biology*, 2, 145–152.

Segers, G., Bradshaw, N., Archer, D., Blissett, K. & Oliver, R.P. (2001) Alcohol oxidase is a novel pathogenicity factor for *Cladosporium fulvum*, but aldehyde dehydrogenase is dispensable. *Molecular Plant-Microbe Interactions*, 14, 367–377.

Shimizu, K. & Keller, N.P. (2001) Genetic involvement of a cAMP-dependent protein kinase in a G protein signaling pathway

regulating morphological and chemical transitions in *Aspergillus nidulans*. *Genetics*, 157, 591–600.
Sidiq, Y., Nakano, M., Mori, Y., Yaeno, T., Kimura, M. & Nishiuchi, T. (2021) Nicotinamide effectively suppresses fusarium head blight in wheat plants. *International Journal of Molecular Sciences*, 22, 2968.
Skogerson, K., Wohlgemuth, G., Barupal, D.K. & Fiehn, O. (2011) The volatile compound BinBase mass spectral database. *BMC Bioinformatics*, 12, 321.
Soldevila, A.I. & Ghabrial, S.A. (2001) A novel alcohol oxidase/RNA-binding protein with affinity for mycovirus double-stranded RNA from the filamentous fungus *Helminthosporium (Cochliobolus) victoriae*: molecular and functional characterization. *Journal of Biological Chemistry*, 276, 4652–4661.
Szewczyk, E., Nayak, T., Oakley, C.E., Edgerton, H., Xiong, Y., Taheri-Talesh, N. et al. (2006) Fusion PCR and gene targeting in *Aspergillus nidulans*. *Nature Protocols*, 1, 3111–3120.
Vicente, V.A., Weiss, V.A., Bombassaro, A., Moreno, L.F., Costa, F.F., Raittz, R.T. et al. (2017) Comparative genomics of sibling species of *Fonsecaea* associated with human chromoblastomycosis. *Frontiers in Microbiology*, 8, 1924.
Wanders, R.J.A., Waterham, H.R. & Ferdinandusse, S. (2016) Metabolic interplay between peroxisomes and other subcellular organelles including mitochondria and the endoplasmic reticulum. *Frontiers in Cell and Developmental Biology*, 3, 83.
Wang, H., Lei, Y., Yan, L., Wan, L., Ren, X., Chen, S. et al. (2016) Functional genomic analysis of *Aspergillus flavus* interacting with resistant and susceptible peanut. *Toxins*, 8, 1–16.
Westrick, N.M., Ranjan, A., Jain, S., Grau, C.R., Smith, D.L. & Kabbage, M. (2019) Gene regulation of *Sclerotinia sclerotiorum* during infection of *Glycine max*: on the road to pathogenesis. *BMC Genomics*, 20, 157.
Westrick, N.M., Smith, D.L. & Kabbage, M. (2021) Disarming the host: detoxification of plant defense compounds during fungal necrotrophy. *Frontiers in Plant Science*, 12, 651716.
Xia, J., Sinelnikov, I.V., Han, B. & Wishart, D.S. (2015) MetaboAnalyst 3.0 – making metabolomics more meaningful. *Nucleic Acids Research*, 43(W1), W251–W257.
Yurimoto, H., Oku, M. & Sakai, Y. (2011) Yeast methylotrophy: metabolism, gene regulation and peroxisome homeostasis. *International Journal of Microbiology*, 2011, 101298.
Zeilinger, S., Gupta, V.K., Dahms, T.E.S., Silva, R.N., Singh, H.B., Upadhyay, R.S. et al. (2016) Friends or foes? Emerging insights from fungal interactions with plants. *FEMS Microbiology Reviews*, 40, 182–207.
Zhang, L. & van Kan, J.A.L. (2013) *Botrytis cinerea* mutants deficient in D-galacturonic acid catabolism have a perturbed virulence on *Nicotiana benthamiana* and *Arabidopsis*, but not on tomato. *Molecular Plant Pathology*, 14, 19–29.
Zhao, T., Havens, W.M. & Ghabrial, S.A. (2006) Disease phenotype of virus-infected *Helminthosporium victoriae* is independent of overexpression of the cellular alcohol oxidase/RNA-binding protein Hv-P68. *Phytopathology*, 96, 326–332.
Zhu, G., Yu, G., Zhang, X., Liu, J., Zhang, Y., Rollins, J.A. et al. (2019) The formaldehyde dehydrogenase *SsFdh1* is regulated by and functionally cooperates with the GATA transcription factor *SsNsd1* in *Sclerotinia sclerotiorum*. *mSystems*, 4, e00397-19.

SUPPORTING INFORMATION

Additional supporting information can be found online in the Supporting Information section at the end of this article.

How to cite this article: Westrick, N.M., Park, S.C., Keller, N.P., Smith, D.L. & Kabbage, M. (2023) A broadly conserved fungal alcohol oxidase (AOX) facilitates fungal invasion of plants. *Molecular Plant Pathology*, 24, 28–43. Available from: https://doi.org/10.1111/mpp.13274